SCIENCE CHINA
Chemistry

• COMMUNICATIONS •
· SPECIAL TOPIC · Metal-Organic Frameworks (MOFs)

August 2016 Vol.59 No.8: 980–983
doi: 10.1007/s11426-016-0071-8

Two highly porous single-crystalline zirconium-based metal-organic frameworks

Wen-Yang Gao[1], Timmy Thiounn[1], Lukasz Wojtas[1], Yu-Sheng Chen[2] & Shengqian Ma[1*]

[1]*Department of Chemistry, University of South Florida, Florida 33620, USA*
[2]*ChemMatCARS, Center for Advanced Radiation Sources, University of Chicago, Illinois 60439, USA*

Received February 11, 2016; accepted April 2, 2016; published online July 14, 2016

Herein we report two highly porous Zr-based metal-organic frameworks (MOFs, **1** and **2**) constructed by the truncated octahedral secondary building unit (SBU) of $Zr_6O_4(OH)_4(CO_2)_{12}$ and the organic linear ligand of 4,4′-stilbenedicarboxylic acid (H_2sbdc) or 4,4′-azobenezenedicarboxylic acid (H_2abdc). Both Zr-based MOFs are obtained as single crystals of suitable size for single-crystal X-ray diffraction analysis. Furthermore, these two Zr-based MOFs have been fully characterized by powder X-ray diffraction (PXRD) studies, thermogravimetric analysis (TGA), infrared spectroscopy (IR) and gas adsorption analysis. In particular, their CO_2 gas adsorption behaviors have been investigated and discussed.

metal-organic frameworks, zirconium cluster, single-crystalline

Citation: Gao WY, Thiounn T, Wojtas L, Chen YS, Ma S. Two highly porous single-crystalline zirconium-based metal-organic frameworks. *Sci China Chem*, 2016, 59: 980–983, doi: 10.1007/s11426-016-0071-8

Metal-organic frameworks (MOFs) [1], composed of polytopic organic ligands linking metal ions or clusters, have been emerging into an important class of porous solid-state materials at an exponential rate over the past two decades [2]. MOFs have thus captured unparalleled attention from both academia and industrial communities due to their structural regularity and synthetic tunability by successful use of crystal engineering and/or reticular chemistry strategies [3–5]. In principal, a structure-designated material can be targeted by judicious selection of the organic ligands and the inorganic secondary building units (SBUs) to match the vertex figures of a given net [6–8]. These intriguing modular features render MOFs to be a prominent platform for various applications in gas storage and separation [9,10], heterogeneous catalysis [11], sensing [12] and other areas [13–15].

Among a variety of inorganic SBUs encountered in MOFs, the zirconium (IV) truncated octahedral SBU, $Zr_6O_4(OH)_4(CO_2)_{12}$ [16], and related expanded analogues [17] have recently been widely employed to construct a series of porous MOFs with high thermal and chemical stability [18–21]. However, it is still difficult to obtain single crystals of Zr-based MOFs, which are large enough for single-crystal X-ray diffraction analysis, tentatively due to the fast formation of high-affinity Zr–O bonds [22]. Herein, we report that two highly porous Zr-based MOFs (**1** and **2**) are constructed by the truncated octahedral SBU of $Zr_6O_4(OH)_4(CO_2)_{12}$ and the organic linear ligand of 4,4′-stilbenedicarboxylic acid (H_2sbdc) or 4,4′-azobenzenedicarboxylic acid (H_2abdc), both of which feature suitable size of single-crystals for single-crystal X-ray diffraction. During the synthesis of these two MOFs, acetic acid is indispensable as the modulator to tune the crystals' size. Furthermore, a thorough characterization of these two Zr-based MOFs has been conducted through powder X-ray diffraction (PXRD) studies, thermogravimetric analysis (TGA), infrared spectroscopy

*Corresponding author (email: sqma@usf.edu)

(IR) and gas adsorption analysis. In particular, their CO_2 gas adsorption behaviors have been investigated and discussed.

The ligand of H_2abdc was synthesized according to the reported procedure [23]. The ligand of H_2sbdc was purchased from TCI (USA). The anhydrous zirconium (IV) chloride ($ZrCl_4$) was purchased from Acros (USA). All solvents were purchased from Fisher Scientific (USA) and used as received. CCDC 1451622 and 1451623 contains the supplementary crystallographic data for this paper. The single-crystal X-ray diffraction data for **1** and **2** were collected at the Advanced Photon Source on beamline 15-ID-B of ChemMatCARS Sector 15 (λ=0.41328 Å, T=100 K). Powder X-ray diffraction (PXRD) patterns were collected using a Bruker D8 Advance X-ray diffractometer (Germany) at 40 kV, 40 mA for Cu-Kα (λ=1.5418 Å) with a scan speed of 0.2 s/step and a step size of 0.02° in the 2θ range of 3° to 50°. Gas adsorption measurements were performed using a Micromeritics ASAP 2020 surface area analyzer (USA). Thermogravimetric analysis (TGA) was performed under nitrogen on a TA Instrument Q50 (USA) from 25 to 800 °C at a speed of 10 °C/min. Fourier transform infrared spectoscopy (FT-IR) data were recorded on a PerkinElmer Spectrum Two instrument (USA) utilizing a range of 4000 to 450 cm^{-1} with a resolution of 4 cm^{-1}. Extended details can refer to the Supporting Information online.

Synthesis of **1**. A mixture of H_2sbdc (68.4 mg, 0.255 mmol), $ZrCl_4$ (60 mg, 0.255 mmol) and *N*,*N*′-dimethylformamide (DMF, 4 mL) with acetic acid (HAc, 0.6 mL) was added into a 20 mL scintillation vial and then heated up to 120 °C for 48 h. The resulting octahedron-shaped colorless crystals of **1** were obtained.

Synthesis of **2**. Follow the similar reaction procedures with that of **1** except using H_2abdc (68.9 mg, 0.255 mmol) instead of H_2sbdc. And the resulting octahedron-shaped orange crystals of **2** were obtained.

Complexes **1** and **2** were synthesized under very similar reaction conditions and relatively large octahedral single-crystals were harvested for single-crystal X-ray diffraction analysis. It is found that acetic acid modulates the MOF synthesis [22]. Acetic acid proved to be essential for the formation of single crystals. Otherwise, only fine powder samples would be obtained. Single-crystal X-ray diffraction (SCXD) analysis reveals that both **1** and **2** crystallize in the same cubic space group, *Fm*-3*m*, with empirical formula of $Zr_6O_4(OH)_4(sbdc)_6$ and $Zr_6O_4(OH)_4(abdc)_6$, respectively. As illustrated in Figure 1, these two Zr-based MOFs are built on the Zr(IV) truncated octahedral SBUs connected by the linear linkers of H_2sbdc and/or H_2abdc, which show the similar connectivity with the well-known UiO series. Basically, each Zr-based SBU is composed of an inner octahedral core, $Zr_6O_4(OH)_4$, alternatively capped by 4 μ_3-O and 4 μ_3-OH groups. All the octahedral edges are bridged by carboxylate groups from the linear linkers, generating a truncated octahedron (connecting the oxygen atoms from twelve carboxylate groups). The truncated octahedral SBUs are linked by H_2sbdc and H_2abdc, forming into the **fcu**-topology extended networks of **1** and **2**. The structure of **1** and/or **2** contains two different types of polyhedral cage cavities: an octahedral cage that is face sharing with 8 tetrahedral cages and edge sharing with 8 additional octahedral cages, as shown in Figure S1 (Supporting Information online).

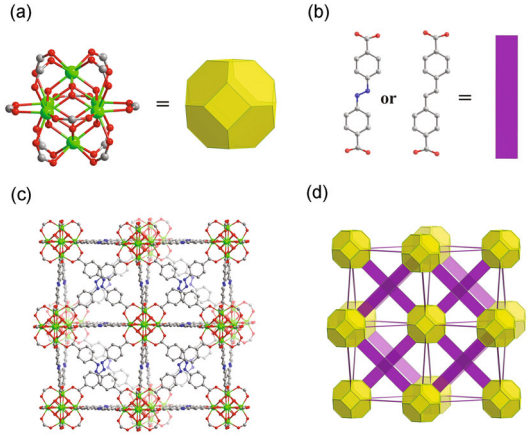

Figure 1 (a) The fundamental secondary building unit (SBU) of **1** and **2** is a six-center octahedral metal cluster, in which eight-coordinate Zr cations are linked via carboxylate ligands; (b) the linear linkers of 4,4′-azobenzenedicarboxylic acid (H_2abdc, left) and 4,4′-stilbenedicarboxylic acid (H_2sbdc, right); (c) the expanded face-centered-cubic network of **2** by connecting the SBUs with abdc linkers; (d) a simplified polyhedral representation of the same network structure of **1** and **2**. The yellow truncated octahedron and purple rectangles correspond, respectively, to Zr_6 cluster coordination polyhedra and linear linkers (color online).

The phase purities of **1** and **2** were verified by PXRD studies, which indicate that the diffraction patterns of the fresh samples are consistent with the calculated ones (Figure S2 and Figure S3). TGA was performed on the fresh samples of **1** and **2** (Figure S4). A continuous weight loss of ~64% from 25 to 170 °C is observed in compound **1**, which corresponds to the loss of guest solvent molecules trapped in the cavities. The plot is followed by a plateau at the range of 170 to 350 °C, before it falls into decomposition. Then the stepwise-like ligand decomposition ends at 560 °C with a weight loss of ~20%. The compound **2** exhibits a similar weight loss process. But the ligand decomposition of **2** happens between 405 and 550 °C. Thus the substantial weight loss in the beginning indicates that these two MOFs demonstrate very high porosity, accommodating a large amount of guest molecules. Moreover, the two Zr-based frameworks also show certain thermal stability. However, compared to UiO-66 [16], the less thermal stability of **1** and **2** can be tentatively attributed to the ligand extension from terephthalic acid to H_2sbdc or H_2abdc.

To examine the permanent porosity of **1** and **2**, gas adsorption studies were performed on the activated samples. The activation conditions are detailed in the Supporting Informa-

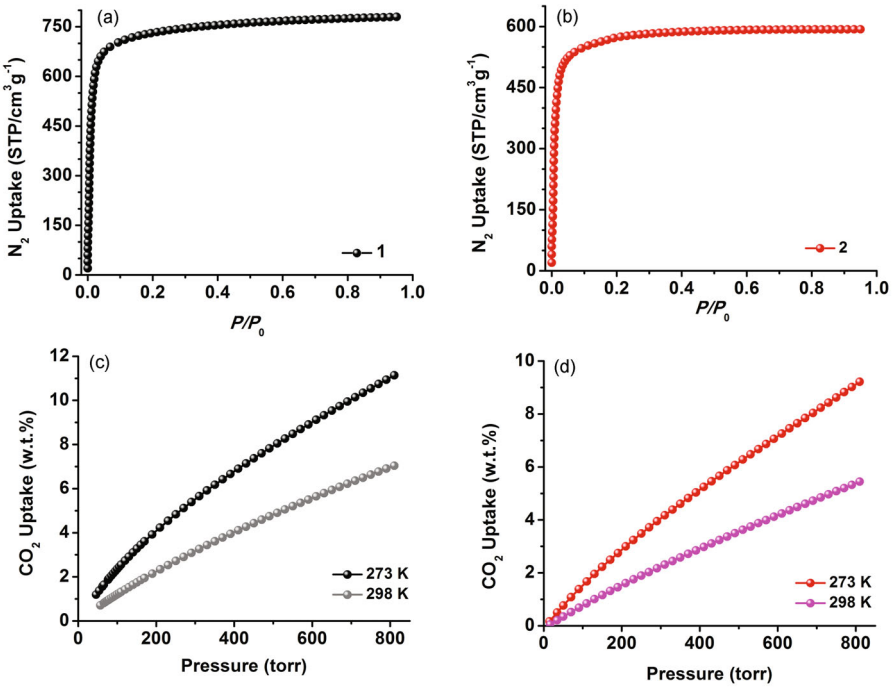

Figure 2 (a) N_2 adsorption isotherm of **1** at 77 K; (b) N_2 adsorption isotherm of **2** at 77 K; (c) CO_2 adsorption isotherms of **1** measured at 273 and 298 K; (d) CO_2 adsorption isotherms of **2** measured at 273 and 298 K (color online).

tion. As shown in Figure 2(a) and (b), the N_2 adsorption isotherms at 77 K for **1** and **2** are observed with uptake capacities of ~780 and ~600 cm³/g, respectively, at the saturation pressure with typical type I adsorption behavior, which is a characteristic of microporous materials. Derived from the N_2 adsorption data, **1** possesses a Brunauer-Emmett-Teller (BET) surface area of ~2890 m²/g (P/P_0=0.0001–0.1) and a corresponding Langmuir surface area of ~3237 m²/g (P/P_0=0.9). Similarly, **2** shows a BET surface area of ~2122 m²/g (P/P_0=0.0001–0.1) and a Langmuir surface area of ~2363 m²/g (P/P_0=0.9). Moreover, density functional theory (DFT) pore size distribution analysis based on the N_2 adsorption data at 77 K indicates that the pore sizes of **1** and **2** are both narrowly distributed at around 13.6 Å, which is in good agreement with the channel width observed in crystal structures (Figure S5 and Figure S6).

Moreover, we evaluated the CO_2 uptake performances of **1** and **2**. As shown in Figure 2(c), **1** can adsorb substantial amounts of CO_2 with a capacity of 10.7 wt% (54.7 cm³/g) at 273 K and 6.77 wt% (34.5 cm³/g) at 298 K under 1 atm pressure. In comparison, **2** demonstrated a lower CO_2 uptake capacity with 8.83 wt% (44.9 cm³/g) at 273 K and 5.20 wt% (26.5 cm³/g) at 298 K under 1 atm pressure, as illustrated in Figure 2(d). Despite the fact that both Zr-based MOFs are characterized by high surface areas, the values of CO_2 uptake capacity under low pressure are very moderate compared to other porous MOFs with open metal centers or Lewis base sites. This can be attributed to the absence of functional sites interacting with CO_2 molecules, which is explained by the relatively low heats of adsorption of CO_2 (21.7 and 18.8 kJ/mol at the initial range, Figure S10) calculated for **1** and **2**.

In summary, two highly porous single-crystalline Zr-based MOFs with **fcu** topology, **1** and **2**, have been built based upon the truncated octahedral SBU of $Zr_6O_4(OH)_4(CO_2)_{12}$ and the linear ligand of H_2sbdc and H_2abdc. Large single-crystals have been obtained by using the modulator of acetic acid. A thorough characterization of these two Zr-based MOFs has been conducted by virtue of SCXD, PXRD, TGA, FT-IR and gas adsorption analysis. In particular, CO_2 gas adsorption behaviors have been described and tentatively interpreted.

Acknowledgments This work was supported by the National Science Foundation (DMR-1352065) and the University of South Florida. ChemMatCARS Sector 15 is supported by the National Science Foundation (NSF/CHE-1346572). This research used resources of the Advanced Photon Source, a U.S. Department of Energy (DOE) Office of Science User Facility operated for the DOE Office of Science by Argonne National Laboratory under Contract No. DE-AC02-06CH11357.

Conflict of interest The authors declare that they have no conflict of interest.

Supporting information The supporting information is available online at chem.scichina.com and link.springer.com/journal/11426. The supporting materials are published as submitted, without typesetting or editing. The responsibility for scientific accuracy and content remains entirely with the authors.

1 Zhou HCJ, Kitagawa S. *Chem Soc Rev*, 2014, 43: 5415–5418
2 Furukawa H, Cordova KE, O'Keeffe M, Yaghi OM. *Science*, 2013, 341: 1230444–1230444
3 Lu W, Wei Z, Gu ZY, Liu TF, Park J, Park J, Tian J, Zhang M, Zhang Q, Gentle III T, Bosch M, Zhou HC. *Chem Soc Rev*, 2014, 43: 5561–5593
4 Desiraju GR. *Crystal Engineering: the Design of Organic Solid.*

Amsterdam and New York: Elsevier Scientific Publishers, 1989
5 Yaghi OM, O'Keeffe M, Ockwig NW, Chae HK, Eddaoudi M, Kim J. *Nature*, 2003, 423: 705–714
6 Gao WY, Ma S. *Commen Inorg Chem*, 2014, 34: 125–141
7 Gao WY, Chrzanowski M, Ma S. *Chem Soc Rev*, 2014, 43: 5841–5866
8 Guillerm V, Kim D, Eubank JF, Luebke R, Liu X, Adil K, Lah MS, Eddaoudi M. *Chem Soc Rev*, 2014, 43: 6141–6172
9 He Y, Zhou W, Qian G, Chen B. *Chem Soc Rev*, 2014, 43: 5657–5678
10 Barea E, Montoro C, Navarro JAR. *Chem Soc Rev*, 2014, 43: 5419–5430
11 Liu J, Chen L, Cui H, Zhang J, Zhang L, Su CY. *Chem Soc Rev*, 2014, 43: 6011–6061
12 Hu Z, Deibert BJ, Li J. *Chem Soc Rev*, 2014, 43: 5815–5840
13 Zhang JP, Liao PQ, Zhou HL, Lin RB, Chen XM. *Chem Soc Rev*, 2014, 43: 5789–5814
14 Qiu S, Xue M, Zhu G. *Chem Soc Rev*, 2014, 43: 6116–6140
15 Han Y, Li JR, Xie Y, Guo G. *Chem Soc Rev*, 2014, 43: 5952–5981
16 Cavka JH, Jakobsen S, Olsbye U, Guillou N, Lamberti C, Bordiga S, Lillerud KP. *J Am Chem Soc*, 2008, 130: 13850–13851
17 Furukawa H, Gándara F, Zhang YB, Jiang J, Queen WL, Hudson MR, Yaghi OM. *J Am Chem Soc*, 2014, 136: 4369–4381
18 Chen Y, Hoang T, Ma S. *Inorg Chem*, 2012, 51: 12600–12602
19 Feng D, Gu ZY, Li JR, Jiang HL, Wei Z, Zhou HC. *Angew Chem Int Ed*, 2012, 51: 10307–10310
20 Liu TF, Feng D, Chen YP, Zou L, Bosch M, Yuan S, Wei Z, Fordham S, Wang K, Zhou HC. *J Am Chem Soc*, 2015, 137: 413–419
21 Morris W, Volosskiy B, Demir S, Gándara F, McGrier PL, Furukawa H, Cascio D, Stoddart JF, Yaghi OM. *Inorg Chem*, 2012, 51: 6443–6445
22 Schaate A, Roy P, Godt A, Lippke J, Waltz F, Wiebcke M, Behrens P. *Chem Eur J*, 2011, 17: 6643–6651
23 Mukherjee PS, Das N, Kryschenko YK, Arif AM, Stang PJ. *J Am Chem Soc*, 2004, 126: 2464–2473